



Electrospun polystyrene fibres on TiO₂ nanostructured film to enhance the hydrophobicity and corrosion resistance of stainless steel substrates

R AZIMIRAD^{1,*} and S SAFA²

¹Malek-Ashtar University of Technology, Tehran, Iran

²Young Researchers and Elite Club, South Tehran Branch, Islamic Azad University, Tehran, Iran

*Corresponding author. E-mail: azimirad@yahoo.com

MS received 14 May 2014; revised 11 November 2014; accepted 15 December 2014

DOI: 10.1007/s12043-015-1021-9; ePublication: 29 August 2015

Abstract. A dual layer of dip-coated TiO₂ film (top layer) and electrospun polystyrene (bottom layer) was coated on stainless steel (SS) substrates. The morphological and structural studies were performed using scanning electron microscopy (SEM) and X-ray diffraction (XRD). Their hydrophobicity and corrosion resistance were also investigated using contact angle (CA) and electrochemical corrosion tests in acidic and salt solutions, respectively. Contact angle results showed that the naturally hydrophilic TiO₂/SS sample (CA ~ 66°) turned into a superhydrophobic surface (CA ~ 148°) when it was covered by polystyrene fibres (PS/TiO₂/SS). This observation can be attributed to the intrinsic hydrophobicity of organic polystyrene fibres (due to their low surface energy) and also to the existence of trapped air bubbles between fibres. Electrochemical corrosion tests showed that the corrosion rate was substantially decreased by using a protective bilayer (PS/TiO₂) from 33 to 0.39 mV/y for bare SS sample and from 0.01 to 0.003 mV/y for PS/TiO₂/SS sample in 1 M salt and acidic solutions, respectively. The superhydrophobic protective layer forms an obstacle against ionic exchange interactions. Therefore, it slows down the breaking of the surface oxidic layer on the metal substrate and prevents the metallic surface underneath from further corrosion.

Keywords. Nanostructures; anticorrosion layers; hydrophobicity; contact angle.

PACS Nos 81.65.–b; 81.65.Kn

1. Introduction

The liquid-repellent surfaces are used in surface-protection applications like waterproof coatings and stain-resistant finishes [1]. The liquid-repellence (or hydrophobicity) of a surface depends on both surface energy and topographical microstructure. It is well known that, the corrosion resistivity can be improved by increasing the hydrophobicity and chemical stability of a surface. Therefore, using suitable layers on sensitive substrates is one of the methods to protect the surface of substrates against corrosive environments. Among various practical applications of the protective layers, corrosion protection of stainless

steel (SS) is very important because steel-based instruments are widely used in pipelines, sea-water structures, ships etc. In these cases, water molecules produce an aqueous electrolyte which facilitates the mobility of corrosive species and so, corrosion rate will substantially increase [2]. Therefore, it is rational to think that the liquid-repellent surfaces can prevent the formation of galvanic cells which improve the anticorrosion properties. In recent years, some literatures have reported the constructive effects of hydrophobicity on corrosion resistivity [3–8]. The two methods that are commonly used for fabricating hydrophobic surfaces are: (a) trapping the air bubbles among the surface hierarchies [9] and (b) coating the surface with intrinsically hydrophobic materials like wax and organic layers [10–14]. Concerning the above-mentioned surface protection mechanisms, various researches have been conducted. For example, Gringard *et al* [15] observed that an electrospun layer of perfluorinated copolymer can considerably strengthen the Al substrate from corrosive ions.

In this paper, we introduce a facile and low-cost method for applying a protective bilayer on SS substrates. This protective bilayer is fabricated from a dip-coated TiO₂ layer and an electrospun polystyrene (PS) microfibrils. Contact angle (CA) measurements indicate that the produced bilayer has superhydrophobic properties (CA ~ 148°).

2. Experimental details

2.1 Synthesis and coating of TiO₂ colloidal solution

The colloidal titanium dioxide suspension was prepared by dissolving tetraisopropyl-orthotitanate (1 g) in 200 ml of ethanol. After 2 h of stirring for hydrolysis reaction, 3 ml HCl (3 M) was added dropwise and the stirring was continued for 30 min [16]. This solution was used as the sol for coating the substrates by dip-coating method. In dip-coating process, STW 24 (DD13)-hot rolled SS substrates were dipped into the solution and withdrawn at a constant rate of 30 mm/min. Then, the samples were annealed at 400°C for 10 min. This procedure was repeated five times to obtain a uniform layer of TiO₂ on the SS substrates.

2.2 Electrospinning of polystyrene on TiO₂/SS

Linear polystyrene (PS) with an average molecular weight (M_w) of 393,400 g/mol (Scientific Polymer Products, Ontario, NY) was dissolved in N,N-dimethylformamide of 12.5 wt% concentration. After preparing a homogeneous sol by stirring, an aluminum foil collector (10 × 10 cm²) was positioned 10 cm from the tip of the needle. The pump was calibrated to achieve a flow rate of 3 ml/h for all the experiments. A potential of 15 kV was applied between the needle and the SS substrate immediately after the formation of a pendant drop at the tip. The electrospinning process was conducted in ambient air at room temperature. The samples fixed on the aluminum foil during electrospinning process were covered by PS microfibrils.

2.3 Characterization methods

The X-ray diffraction patterns of the samples were measured using a Philips X'pert instrument operating with Cu-K α radiation ($\lambda = 1.54178 \text{ \AA}$) at 40 kV/40 mA. A small amount

of the coated TiO₂ was mechanically scratched and depicted by a Philips 400T transmission electron microscope (TEM) operating at 80 kV. A TESCAN VEGA scanning electron microscope (SEM) was also used for evaluating the morphology and thickness of the samples. A thin film of gold was coated over the SEM samples by a desktop sputtering system (Nanostructured Coating Co., Iran). Contact angle measurements were performed in air at room temperature two weeks after the sample was prepared using a home-made contact angle meter with $\pm 1^\circ$ accuracy. Two microlitres of water droplets were injected on several spots of the sample surface using a microlitre injector.

2.4 Corrosion characterization

The salt corrosion resistance of the samples was measured in a 1 M NaCl aqueous solution at room temperature, by means of Autolab electrochemical system (PGSTAT302N) with 0.5 mV/s. Similar tests were done for evaluating the acidic resistivity of the samples in

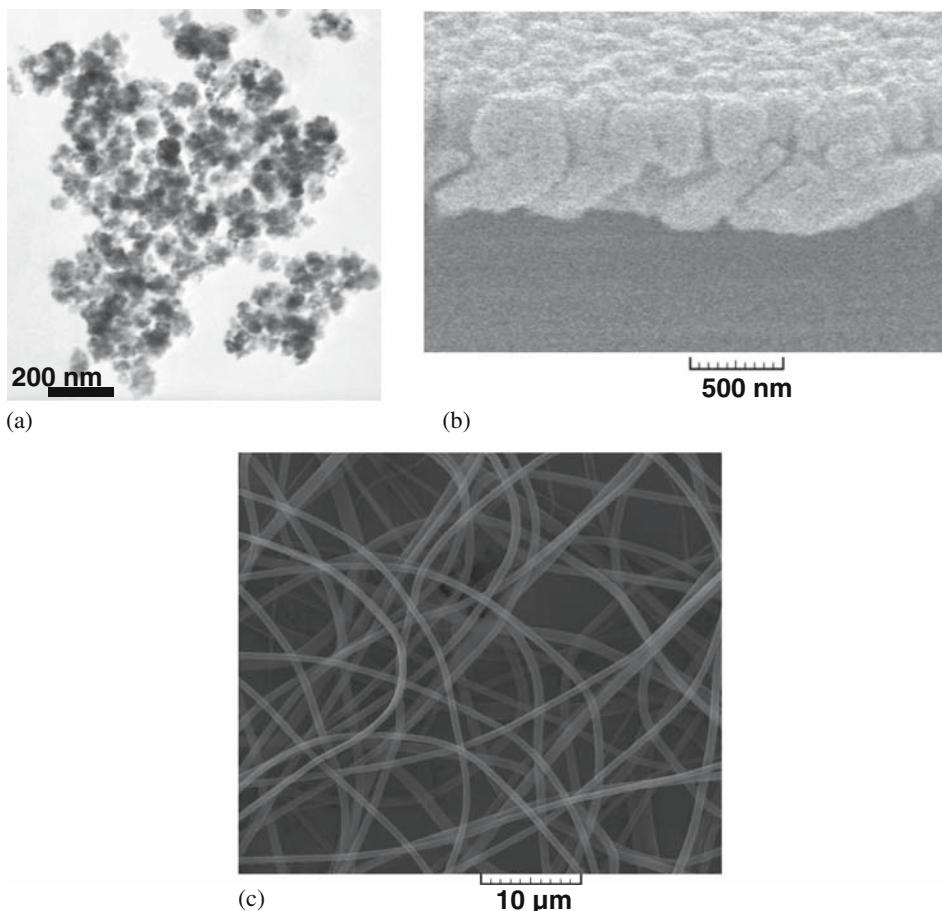


Figure 1. (a) TEM image of the scratched TiO₂ film, (b) SEM image of the cross-section of the TiO₂ film and (c) the PS fibres.

1 M H_2SO_4 solution. The salt spray experiments were performed to form corrosion scales over the samples. Different rectangular shaped samples (7 cm width and 5 cm length) were kept for 24 h at 35°C with a spray of 8 wt% salt water solution.

3. Results and discussion

TEM image of the scratched TiO_2 film is shown in figure 1a. This figure shows that the sample consists of nanoparticles having sizes smaller than 50 nm. The cross-section of the TiO_2 film is illustrated in figure 1b. As can be seen, the dip-coated TiO_2 film is formed from the uniform columnar islands with a thickness of about 500 nm on the surface of the SS substrate. Afterwards, PS fibres were electrospun on the TiO_2 film. The morphology and size of the fibres are shown in figure 1c. As can be seen, the PS fibres with diameter of less than $1\ \mu\text{m}$ and length of a few millimeters woven together, completely covered the underneath layer.

XRD pattern of the TiO_2 film is shown in figure 2 which indicates that the dip-coated film is crystallized in anatase phase. The typical diffraction peaks at $2\theta = 25.3, 36.9, 37.8, 48.0, 55.1$ and 68.8° are assigned to the (1 0 1), (1 0 3), (0 0 4), (2 0 0), (2 1 1) and (1 1 6) planes of the anatase phase, respectively [17]. Relatively large width of the anatase peaks and the lack of any other peaks reveal that a high purity TiO_2 film is nanocrystallized on the surface of the substrate.

The contact angle measurements of the samples show that the TiO_2/SS sample is hydrophilic while the $\text{PS}/\text{TiO}_2/\text{SS}$ sample is completely superhydrophobic (see figure 3). This amazing superhydrophobicity can be explained by the intrinsic hydrophobicity of the PS fibres due to the very low surface energy of the PS [18] and the existence of the trapped air bubbles between microfibrils [19]. Microfibrils naturally create microcavities between themselves (see figure 1c) which can trap air bubbles. The trapped bubbles facilitate water droplet sliding over the surface and this phenomenon can be explained using Cassie-Baxter interface model [20].

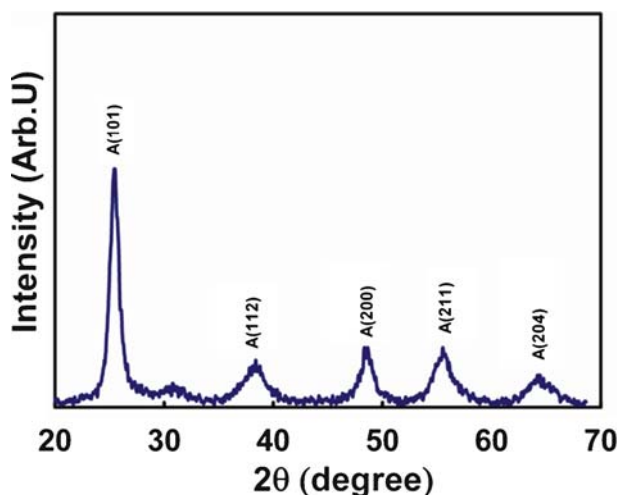


Figure 2. XRD pattern of the dip-coated TiO_2 film.

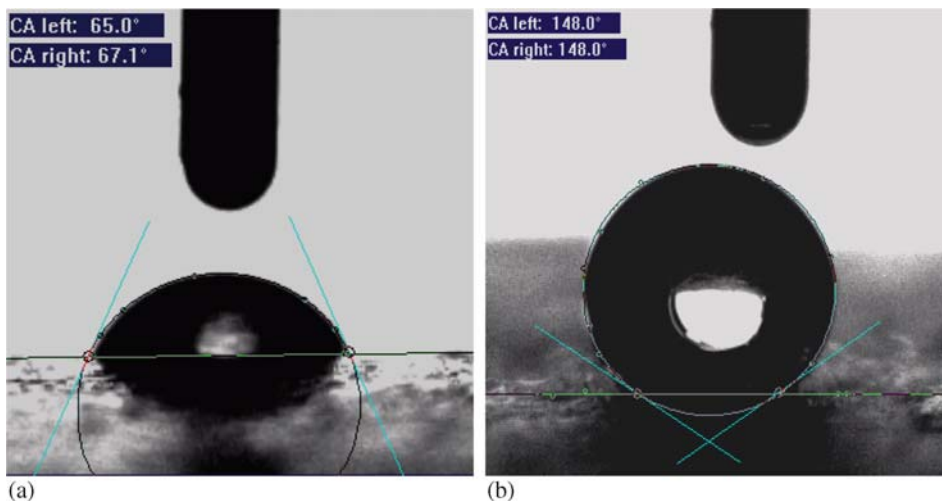


Figure 3. Results of contact angle measurements for (a) TiO₂/SS and (b) PS/TiO₂/SS samples.



Bare steel before salt spray



Bare steel after 24 h immersion



TiO₂/steel after 24 h immersion



SP/TiO₂/steel after 24 h immersion

Figure 4. Optical images of the different samples after salt spray process.

Figure 4 shows the photographs of different samples after immersing them in the salt spray chamber for about 24 h as compared to the bare SS before the salt spray. As can be seen, the bare SS is completely colourized as iron oxide. The TiO₂/SS sample is partially

corroded during the test and red strips appeared on the surface of the sample. But, the superhydrophobic PS/TiO₂/SS sample is nearly unchanged. This result clearly demonstrates the good corrosion protection of the prepared coating under the salt spray condition.

Potentiodynamic polarization curves of the samples in different solutions are shown in figure 5 and their parameter are summarized in table 1. As can be seen, the trend of current density in both acidic and salt solutions is as follows: SS > TiO₂/SS > PS/TiO₂/SS. The lowest corrosion current density and therefore, the lowest anode dissolution as well as the best corrosion protection behaviour are obtained for the PS/TiO₂/SS sample which is in good agreement with previous results (figure 4). It is known that the surface defects (small pores or cracks and grain boundaries) are responsible for corrosion because of the formation of the local galvanic and crevice cells [21]. For the sample covered by the bilayer, the protective TiO₂ barrier layer covers the surface defects and the superhydrophobic electrospun PS layer acts as an insulator against the formation of the galvanic and crevice cells [22,23]. Moreover, the corrosion rates were calculated by assuming a uniform corrosion over time. As can be seen from table 1, corrosion rates in the salt and acidic solutions are decreased from 33 and 0.39 mV/y for the bare SS sample to 0.01 and 0.003 mV/y for the PS/TiO₂/SS sample, respectively.

Recently, Mohamed *et al* [24], similar to our results, observed that the superhydrophobic coatings form a strong resistive layer which slows down the breaking of the up-surface

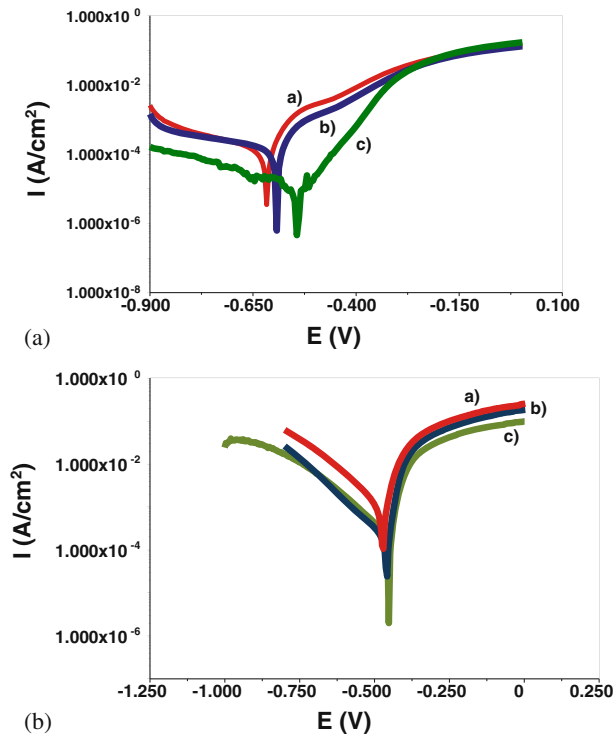


Figure 5. Potentiodynamic polarization curves of the bare SS (Curve a), TiO₂/SS (Curve b) and PS/TiO₂/SS (Curve c) in the (a) NaCl (1 M) and (b) H₂SO₄ (1 M) solutions.

Table 1. Potentiodynamic polarization parameters of different samples in salt and acidic solutions.

Sample	Environment	E_{corr} (mV)	I_{corr} ($\mu\text{A}/\text{cm}^2$)	Corrosion rate (mV/y)
SS	NaCl (1 M)	-0.62	27	33
	H ₂ SO ₄ (1 M)	-0.47	34.2	0.39
TiO ₂ /SS	NaCl (1 M)	-0.59	3.3	0.03
	H ₂ SO ₄ (1 M)	-0.45	5.1	0.05
PS/TiO ₂ /SS	NaCl (1 M)	-0.54	1.1	0.01
	H ₂ SO ₄ (1 M)	-0.44	0.02	0.003

compact oxide layer on metal substrates and thus, prevents the underneath metallic surface from further corrosion. Several other works have also been carried out to study the corrosion resistance of metals coated with the superhydrophobic surfaces. Yin *et al* [25] prepared a stable superhydrophobic film by mystic (fatty) acid (chemically adsorbed onto the anodized aluminum substrate). The contact angle of the prepared sample was about 154° and its corrosion resistance in seawater was improved significantly. De Leon *et al* [26] coated stable superhydrophobic layer of polythiophene on SS substrates using a very simple dip-coating method. Their results showed that in the presence of superhydrophobic surface, the anodic corrosion potential was shifted towards higher values and the anodic and cathodic corrosion currents were significantly reduced. This improvement in anticorrosion property of SS can considerably increase its potential applications, especially in marine industries.

4. Conclusions

A bilayer of dip-coated TiO₂ film (bottom layer) and electrospun polystyrene (top layer) was coated on to a stainless steel substrate. Contact angle results showed that the naturally hydrophilic TiO₂/SS sample (CA ~ 66°) turned into a superhydrophobic surface (CA ~150°) when it was covered by polystyrene fibres (PS/4TiO₂/SS sample). This can be attributed to the intrinsic hydrophobicity of organic polystyrene fibres (due to their low surface energy) and the existence of trapped air bubbles between the fibres. Photographic images before and after corrosion test in the salt spray test revealed that the surface of the PS/TiO₂/SS sample within 24 h was still intact. In contrast, the bare SS sample was completely oxidized to iron oxide. The electrochemical results confirmed these results and showed that the corrosion rates of the sample in the salt and acidic solutions were substantially decreased from 33 and 0.39 mV/y for bare SS to 0.03 and 0.05 mV/y for SS/TiO₂ and 0.01 and 0.003 mV/y for PS/TiO₂/SS, respectively. The superhydrophobic coating forms an obstacle against ionic exchange which slows down the breaking of surface oxide layer and thus, prevents the underneath metallic surface from further corrosion. This approach enables the promising prospect that a variety of functional hybrid materials with anticorrosion properties will be accessible for widespread marine applications.

Acknowledgement

The authors would like to thank the Iran National Science Foundation for supporting the work.

References

- [1] L Huang, S P Lau, H Y Yang, E S P Leong, S F Yu and S Prawer, *J. Phys. Chem. B* **109**, 7746 (2005)
- [2] M Y P Sengupta, M D Blanton and James W Rawlins, In: *The Waterborne Symposium: Proceedings of the Thirty-Ninth Annual International Waterborne, High-Solids, and Powder Coatings Symposium* (New Orleans, Louisiana, 2012) DEStech Publications, Inc., p. 150
- [3] J R Blachere, *High temperature corrosion of ceramics*, No. DOE/ER/45117-2 (Pittsburgh Univ., PA, USA, 1986)
- [4] A F Azevedo, E J Corat, N G Ferreira and Vladimir J Trava-Airoldi, *Surf. Coat. Technol.* **194**, 271 (2005)
- [5] G X Shen, Y C Chen, L Lin, C J Lin and D Scantlebury, *Electrochim. Acta* **50**, 5083 (2005)
- [6] Y Yin, T Liu, Shougang Chen, Tong Liu and Sha Cheng, *Appl. Surf. Sci.* **255**, 2978 (2008)
- [7] S Yuan, S O Pehkonen, Bin Liang, Y P Ting, K G Neoh and E T Kang, *Corros. Sci.* **53**, 2738 (2011)
- [8] C Hsieh, J-M Chen, R-R Kuo, T-S Lin and C-F Wu, *Appl. Surf. Sci.* **240**, 318 (2005)
- [9] A Checco, T Hofmann, E DiMasi, C T Black and B M Ocko, *Nano Lett.* **10**, 1354 (2010)
- [10] C H Xue, S-T Jia, J Zhang and J-Z Ma, *Sci. Technol. Adv. Mater.* **11**, 033002-1 (2010)
- [11] C H Xue, S-T Jia, J Zhang and L-Q Tian, *Thin Solid Films* **517**, 4593 (2009)
- [12] B Balu, Victor Breedveld and Dennis W Hess, *Langmuir* **24**, 4785 (2008)
- [13] X M Li, D Reinhoudt and M Crego-Calama, *Chem. Soc. Rev.* **36**, 1350 (2007)
- [14] B Cortese, S D'Amone, M Manca, I Viola, R Cingolani and G Gigli, *Langmuir* **24**, 2712 (2008)
- [15] B Grignard, A Vaillant, J D Coninck, M Piens, A M Jonas, C Detrembleur and Christine Jerome, *Langmuir* **27**, 335 (2010)
- [16] O Akhavan, R Azimirad, S Safa and M M Larijani, *J. Mater. Chem.* **20**, 7386 (2010)
- [17] H Tang, K Prasad, R Sanjines, P E Schmid and F Levy, *J. Appl. Phys.* **75**, 2042 (1994)
- [18] X Lu, J Zhou, Y Zhao, Y Qiu and J Li, *Chem. Mater.* **20**, 3420 (2008)
- [19] Y Xiu, L Zhu, D W Hess and C P Wong, *Nano Lett.* **7**, 3388 (2007)
- [20] A B D Cassie and S Baxter, *Trans. Faraday Soc.* **40**, 546 (1944)
- [21] M M Larijani, M Elmi, M Yari, M Ghoranneviss, P Balashabadi and A Shokouhy, *Surf. Coat. Technol.* **203**, 2591 (2009)
- [22] M A Schubert, *Impact modified polystyrene seals for galvanic cells*, U.S. Patent 6,306,537, issued October 23, 2001
- [23] A Mirmohseni and A Oladegaragoze, *Synth. Met.* **114**, 105 (2000)
- [24] A Mohamed, A M Abdullah and N A Younan, *Arabian J. Chem.* (2014) (In press), <http://dx.doi.org/10.1016/j.arabjc.2014.03.006>
- [25] Y Yin, T Liu, S Chen, T Liu and S Cheng, *Appl. Surf. Sci.* **255**, 2978 (2008)
- [26] A C de Leon, R B Pernites and R C Advincula, *ACS Appl. Mater. Interfaces* **4**, 3169 (2012)